

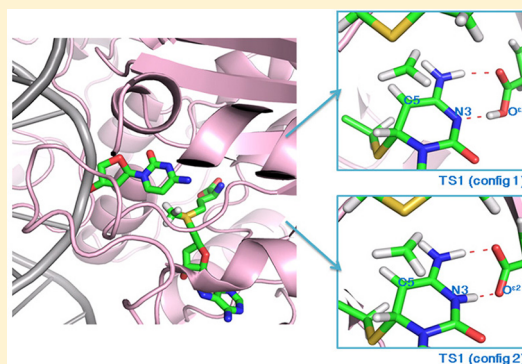
DNA Cytosine Methylation: Structural and Thermodynamic Characterization of the Epigenetic Marking Mechanism

Jin Yang,[§] Lee Lior-Hoffmann,^{§,†} Shenglong Wang,[§] Yingkai Zhang,^{*,§} and Suse Broyde^{*,†}

[§]Department of Chemistry, and [†]Department of Biology, New York University, New York, New York 10003, United States

S Supporting Information

ABSTRACT: DNA cytosine methyltransferases regulate the expression of the genome through the precise epigenetic marking of certain cytosines with a methyl group, and aberrant methylation is a hallmark of human diseases including cancer. Targeting these enzymes for drug design is currently a high priority. We have utilized ab initio quantum mechanical/molecular mechanical (QM/MM) molecular dynamics (MD) simulations to investigate extensively the reaction mechanism of the representative DNA methyltransferase *HhaI* (*M.HhaI*) from prokaryotes, whose overall mechanism is shared with the mammalian enzymes. We obtain for the first time full free energy profiles for the complete reaction, together with reaction dynamics in atomistic detail. Our results show an energetically preferred mechanism in which nucleophilic attack of cytosine C5 on the S-adenosyl-L-methionine (AdoMet) methyl group is concerted with formation of the Michael adduct between a conserved Cys in the active site with cytosine C6. Spontaneous and reversible proton transfer between a conserved Glu in the active site and cytosine N3 at the transition state was observed in our simulations, revealing the chemical participation of this Glu residue in the catalytic mechanism. Subsequently, the β -elimination of the C5 proton utilizes as base an OH[−] derived from a conserved crystal water that is part of a proton wire water channel, and this *syn* β -elimination reaction is the rate-limiting step. Design of novel cytosine methylation inhibitors would be advanced by our structural and thermodynamic characterization of the reaction mechanism.



The DNA methyl transferases play critical roles in many biological functions. They are key players in regulating gene expression:¹ in embryonic development,^{2,3} in X-chromosome inactivation,⁴ in genomic imprinting,⁵ and, overall, in epigenetic mechanisms that transmit genetic information without altering the actual base sequence of the DNA through regulation of the methylation status.^{6–8} Aberrant methylation is a feature of cancers and other diseases.^{9–11} Methyl transferase activity is impaired by DNA damage resulting from environmental carcinogens, notably benzo[*a*]pyrene,^{12,13} and methylation status has an important impact on the reactivity of DNA with benzo[*a*]pyrene metabolites.¹⁴ The design of methylation inhibitors is an active current research frontier.^{15–19} Understanding the mechanism for the methyl transfer reaction in atomistic detail would advance drug design and could provide novel opportunities for regulating gene expression through control of the methylation process.

We focus here on the very well-studied prokaryotic cytosine methyltransferase *HhaI* (*M.HhaI*) which carries out the enzymatic process for methylation of cytosine C5 in DNA. Like all methyltransferases it uses S-adenosyl-L-methionine (AdoMet) as the methyl donor and flipping of the target base into a pocket of the enzyme. It has been established based on numerous investigations that the catalytic process entails nucleophilic attack of cysteine 81 (Cys81) of this enzyme on the cytosine C6 to form a covalent adduct via Michael addition; this adduct promotes the nucleophilicity of the cytosine C5 for

attack on the AdoMet methyl group,²⁰ and subsequently, the C5 proton is abstracted via a β -elimination reaction.^{6,21} The mammalian enzymes employ a similar mechanism,^{6,8,22} which has recently been substantiated with a crystal structure of a productive covalent DNMT1–DNA complex.²³ It is notable that this crystal structure reveals a covalent adduct between a conserved cysteine and C6 of the target cytosine, as had been observed crystallographically with the prokaryotic enzyme, including some examples containing incorporated nucleoside inhibitor drugs in place of the cytosine.^{24–26} It is also worth noting that DNMT1 is a maintenance methyltransferase, and in this case the mechanism for maintenance and de novo methyltransferases such as *M.HhaI* are similar; hence, new mechanistic insights could be relevant to drug design for inhibition of both methyltransferases.

Current DNA methyltransferase inhibitors generally fall into two categories: nucleoside analogues and non-nucleoside inhibitors. The nucleoside analogues become incorporated in the DNA and may function by inhibiting methylation or β -elimination, but they form the Michael adduct and thus act as covalent inhibitors. Two nucleoside analogue inhibitors are currently in use, azacytidine and decitabine, employed to treat

Received: February 8, 2013

Revised: March 25, 2013

Published: March 26, 2013

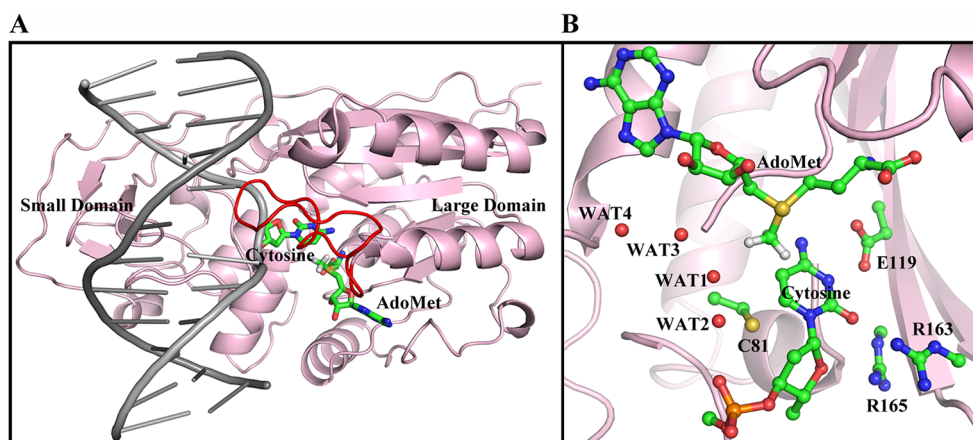


Figure 1. (A) Ternary structure of *HhaI* methyltransferase (PDB ID:³⁸ 6MHT). The flipped out cytosine and the cofactor AdoMet are colored by atom. The protein is pink. The large and small domains are indicated. The DNA is gray and the catalytic loop is red. (B) The active site, including the target cytosine, catalytic Cys81 from the catalytic loop, Glu119, Arg163, and Arg165 from the large domain and the cofactor AdoMet are shown, and crystal waters are indicated. The active site structure was remodeled from the crystal structure as described in Computational Methods.

myelodysplastic syndrome. The non-nucleoside inhibitors bind DNA methyltransferases and exert their inhibitory effects through a variety of different mechanisms.²⁷

At present, a full atomistic, thermodynamic, and dynamic characterization of the chemical reaction process remains to be determined. Questions that remain not fully resolved include whether the methylation reaction is concerted or stepwise, the specific roles of certain key amino acids in the active site, the nature of the base that abstracts the C5 proton, the role of waters in the chemical process, and the energetics and dynamics of the bond forming and breaking events. Previous computational studies^{28,29} for this enzyme system did not obtain free energies or take the enzyme dynamics into account and either used the semiempirical density functional based tight binding (DFTB) approach as the quantum mechanical method²⁸ or treated the heterogeneous enzyme environment with an implicit continuum solvent model.²⁹

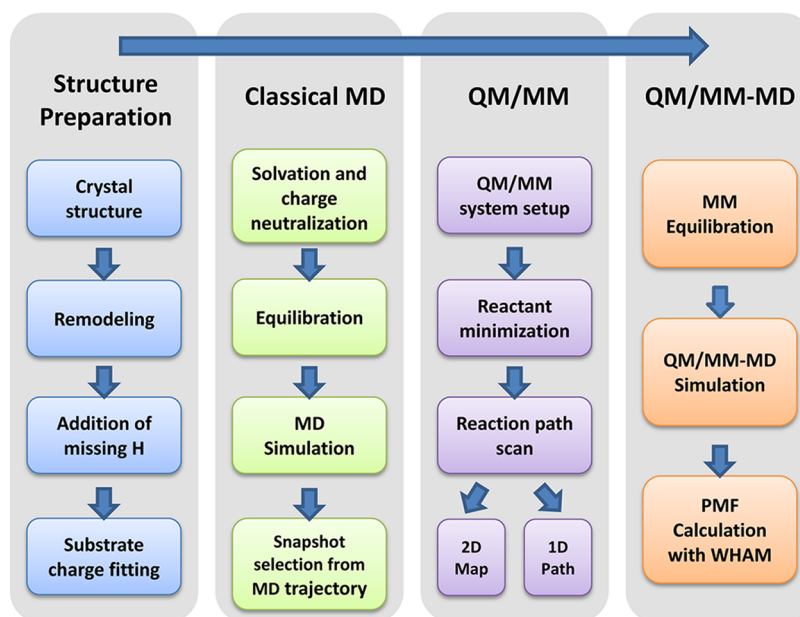
We have utilized Born–Oppenheimer ab initio QM/MM-MD calculations to investigate the mechanism for the methyl transfer reaction in *M.HhaI*; the chemically reacting moieties are described by the ab initio QM method, the surrounding enzyme and aqueous environment are treated explicitly by classical MM, and the enzyme active site dynamics and those of the surroundings are simulated on an equal footing. This approach now has the power to robustly elucidate the full course of the chemical steps in enzyme mechanisms.^{30–36} We explored many mechanistic issues that remain under consideration and thoroughly investigated a variety of plausible reaction schemes. Our extensive computational investigations resulted in a preferred methyl transfer mechanism for *M.HhaI*. This mechanism involves nucleophilic attack of deprotonated Cys81 thiolate on the cytosine C6, concerted with methyl transfer. Subsequently, an OH[−], derived through a proton wire to surface water and involving crystal and solvent waters, serves as the base to abstract the C5 proton. Our results provide complete free energy profiles for the reaction mechanism, reaction barriers and transition state and intermediate structures for both methylation and proton abstraction steps; our extensive investigations of possible bases support the previous mechanistic suggestion²⁸ that the OH[−] is likely to be the proton-abstracting base and that proton abstraction is chemically rate-determining. We obtain atomistic and dynamic

views of the bond breaking and forming processes, which reveal the intricate dynamic interplay between formation of the Michael adduct and the methyl transfer step. We also resolve uncertainties in the role of Glu119 in the active site: it forms a hydrogen bond with cytosine N3 at the reactant and at the transition state where the proton spontaneously and reversibly oscillates between being bonded to Glu and to cytosine N3. Hence, the chemical participation of the Glu in the reaction mechanism is manifested. Thus, our study for the first time fully characterizes the *HhaI* methyltransferase reaction, provides new molecular insights on experimental data,^{20,24,37} and more broadly is very likely applicable to the critical human cytosine methylation enzymes that are key in governing epigenetic inheritance, since mammalian DNMT1 relies on a similar chemical mechanism.²³

■ COMPUTATIONAL METHODS

Initial Preparation. The initial structure of the enzyme-reactant complex was constructed based on a ternary crystal structure of the DNA methyltransferase *M.HhaI* with *S*-adenosyl-L-methionine (AdoMet) and DNA (PDB ID:³⁸ 6MHT) (Figure 1).³⁹ The critical methylation target sequence is 5′-GC*GC-3′/3′-CG C′G-5′, with C* as the target for methylation by AdoMet. In this structure, the O4′ of the target cytosine has been replaced by a sulfur atom (4′-thio-2′-deoxycytidine) in an effort to inhibit the methylation reaction. In addition, the DNA was hemimethylated, with a methyl group on C′. Despite the presence of the 4′ thiol, partial reaction did take place, and two sets of coordinates were presented for the methyl group and the sulfur of Cys81: in one set, the methyl remained on the AdoMet and the sulfur on Cys81, while in the second set the methyl had transferred to the cytosine C5, and the sulfur of Cys81 was partially bonded to C6 of cytosine. We selected the former set of coordinates for our study, and we remodeled the sulfur atom on the sugar as the natural oxygen. Since we wished to investigate de novo methylation, requiring a prechemistry system containing unmethylated DNA and AdoMet, we replaced the methyl on C′ with a hydrogen atom. No crystal structure of such a prechemistry system without mutation appears to be yet available for *M.HhaI*; the structure we selected for this study had the highest resolution (2.05 Å) of any available *M.HhaI* crystal structure containing the AdoMet.

Scheme 1. Computational Protocol



The molecular modeling was performed with Discovery Studio (Accelrys Software, Inc.). Hydrogen atoms were added to this model of the enzyme–substrate complex by the LEAP module of the AMBER 10 simulation package.⁴⁰ The protonation states of charged residues were computed by the H++^{41,42} and pdb2pqr⁴³ programs. In addition, we considered the potential H-bonding network, solvent exposure of the ionizable residues, potential steric clashes if the proton was added, and preservation of the crystal structure in assigning protonation states. The assignments that we made are given in Table S1 (Supporting Information).

The initial model was subjected to 4 ns of MD simulations using AMBER 10.⁴⁰ We employed the Amber99SB^{44–46} force field with modification for DNA by parmbsc0.⁴⁷ Bond length, bond angle, torsional and van der Waals parameters for the methyl donor AdoMet were taken from Markham et al.⁴⁸ Partial atomic charges for the AdoMet were calculated by using Hartree–Fock quantum mechanical calculations with 6-31G* basis set^{49,50} without geometry optimization, employing the Gaussian 03 package from Gaussian, Inc.⁵¹ The charges were then fitted to each atomic center with the RESP algorithm.⁵² The fitted charges are shown in Table S2 (Supporting Information). The structure was neutralized by 20 Na⁺ counterions and was solvated with a periodic rectangular box of TIP3P water^{53,54} with 10 Å buffer around the enzyme–substrate complex. The total number of atoms in the system was ~60 453, of which ~54 432 were water molecules. Details of the MD protocols are given in Supporting Information. The final snapshot from the stable 4 ns trajectory was utilized for the subsequent QM/MM calculations. PyMOL (Schrödinger, LLC) was employed to make molecular images and movies.

Born–Oppenheimer Ab Initio QM/MM-MD Simulation. In the QM/MM calculations, the enzyme substrate model prepared as described above was partitioned into QM subsystem and MM subsystem, in which all components that participated in chemical reactions are included in the QM region, as illustrated in Figure S1 of Supporting Information. The QM subsystem was treated by the hybrid density functional B3LYP^{55–57} with a medium split valence basis set

and polarization functions 6-31G*. The QM/MM interface was described by a pseudobond approach.^{58–60} All other atoms were described classically. To reduce computational cost for the MM calculations during the QM/MM simulation process, spherical boundary conditions were utilized: the C5 atom of cytosine at the active site was selected as the center, and atoms that were 20.0 Å away from the C5 atom were fixed during the simulation. Solvent water molecules with a distance from the C5 atom greater than 30.0 Å were removed. The prepared system had ~12 779 atoms in total, which included 6001 protein atoms, 2258 water molecules, and 4 Na⁺ counterions. All QM/MM and QM/MM-MD calculations were carried out with modified versions of the Q-Chem⁶¹ and Tinker programs.⁶² After the partition of the QM and MM subsystem, the entire reactant system was minimized first by an iterative optimization procedure. Then an iterative minimization procedure with the reaction coordinate driving method⁶³ was employed to map out a minimum energy path with ab initio QM/MM calculations. For each determined structure along the reaction path, an MD simulation of the MM subsystem with the MM force field was further carried out for 500 ps with the frozen QM subsystem. The resulting snapshots were used as starting structures for Born–Oppenheimer ab initio QM/MM-MD simulations with umbrella sampling^{30,64,65} that applies a harmonic potential to constrain the reaction coordinate (RC) at successive values. In order to ensure sufficient overlap between the successive windows, force constants in the range of 40–100 kcal·mol^{−1}·Å^{−2} were employed. We sampled 30 ps for each window. For these biased QM/MM-MD simulations, the Beeman algorithm⁶⁶ was used to integrate the Newton equations of motion with a time step of 1 fs. Cutoffs of 18 and 12 Å were employed for electrostatic and van der Waals interactions between the MM atoms, respectively. There was no cutoff for electrostatic interactions between the QM and MM regions. Configurations of 25 ps were collected for data analysis after a 5 ps QM/MM-MD equilibration. Finally, the probability distributions of each window were determined and pieced together with the weighted histogram analysis method (WHAM)^{67–69} to obtain free energy profiles. This computa-

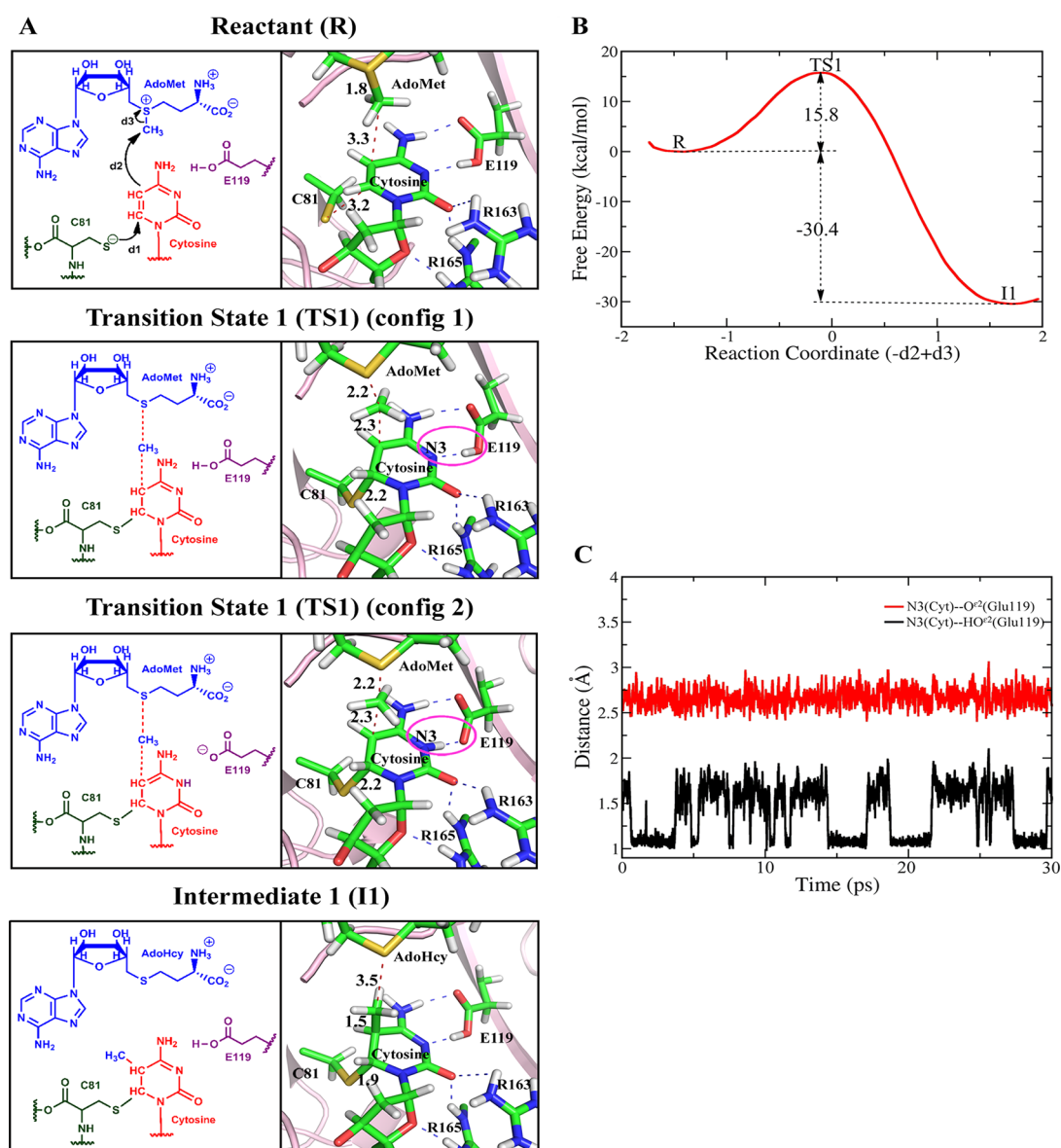


Figure 2. (A) Mechanism for the methyl transfer reaction catalyzed by *M.HhaI* involving concerted methyl transfer and covalent bonding of Cys81–S[−] with C6 of cytosine. Key structures of the obtained mechanism with bond distances are shown. Blue dashed lines indicate hydrogen bonds. Red dashed lines denote key distances. (B) Free energy profile. The potential energy profile and bond length analyses are shown in Figure S2 of Supporting Information. (C) Distance between cytosine N3 and HO² of Glu119 (black) and the distance between cytosine N3 and O² of Glu119 (red) in the QM/MM-MD simulation; there are two configurations at the transition state 1 (TS1) with Glu119 hydrogen oscillating between being covalently linked to cytosine N3 and Glu119. These are circled in 2A. See Movie S1 of Supporting Information.

tional protocol (Scheme 1) has been demonstrated to be feasible and successful in several enzyme investigations.^{30–36}

RESULTS

We have made an extensive exploration of the *M.HhaI* catalyzed methyl transfer reaction, utilizing state-of-the-art ab initio QM/MM-MD simulations. We investigated many reaction schemes. For each scheme, we calculated the minimum energy path or the two-dimensional minimum potential energy surface, employing the reaction coordinate driving method and B3LYP (6-31G*) QM/MM computations. The most promising schemes derived from the one- or two-dimensional searches were further investigated with B3LYP (6-31G*) QM/MM-MD simulations with umbrella sampling. Numerous mechanistic paths could be examined through this hierarchy of strategies.

We were motivated to apply this robust methodology to this enzyme system because it is a well-studied representative of DNA methyltransferases, which share catalytic mechanistic features^{6,8} with mammalian DNMT1.²³ The extensive literature including kinetic studies,^{20,37,70} X-ray crystal structures,^{24,25,39,71,72} and studies of mutant enzymes^{73–75} have implicated conserved residues^{76,77} Cys81, Glu119, Arg163, and Arg165 in the catalytic process. Cys81 is understood to form a covalent bond with cytosine C6 to activate the cytosine C5 for nucleophilic attack on the methyl group of cofactor AdoMet.^{6,20,21} However, the literature contains varied perspectives on certain key mechanistic issues.

We have therefore investigated a number of mechanistic possibilities for the methyl transfer reaction. (**M1**): Concerted methyl transfer and covalent bonding of Cys81–S[−] with C6 of cytosine (Figure 2).²⁸ (**M2**): Stepwise methyl transfer; covalent

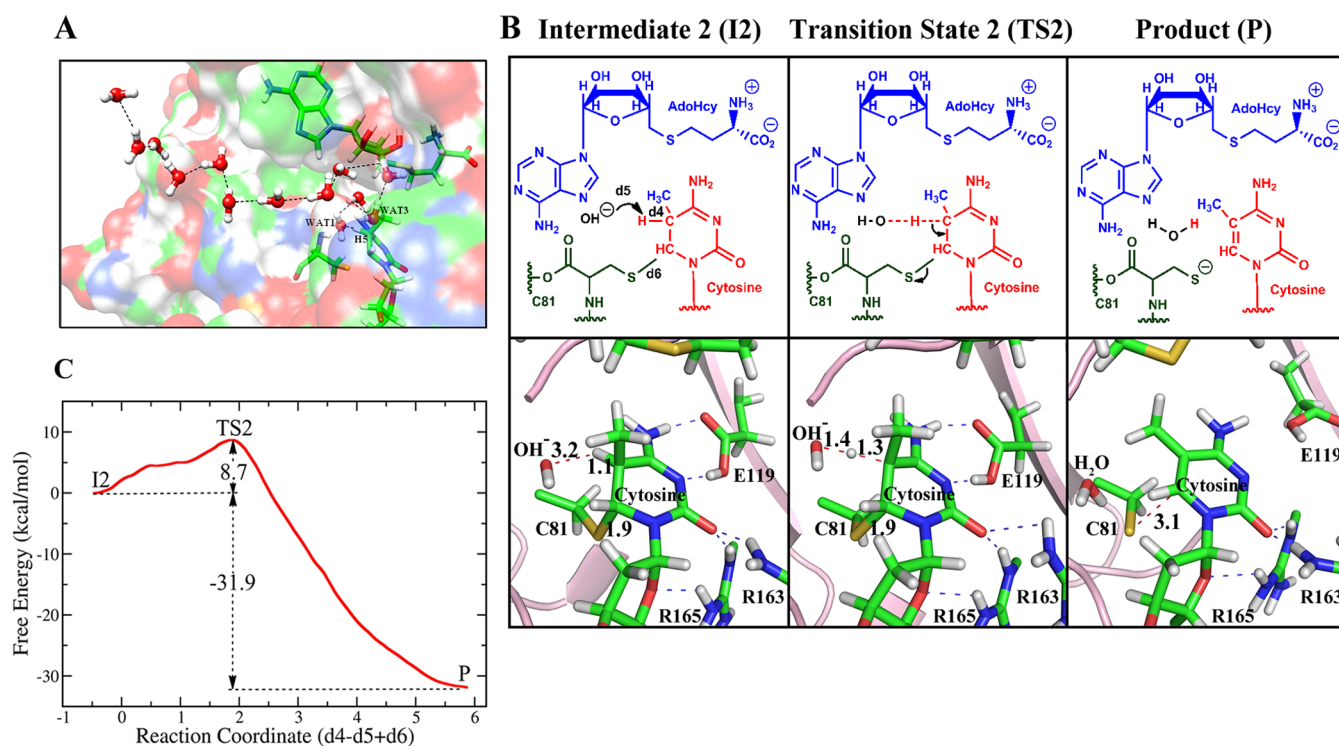


Figure 3. Mechanism for the proton β -elimination reaction catalyzed by *M.HhaI*. (A) A proton wire provides a OH^- as the base to abstract the cytosine C5 proton (H5). The chain of water molecules connecting to surface bulk water is shown by dashed lines. WAT1 and WAT3 are at the sites of the respective crystal waters shown in Figure 1B and WAT1 provides the OH^- . (B) The mechanism with the key structures and distances denoted. The blue dashed lines are hydrogen bonds. Red dashed lines denote key distances. (C) Free energy profile. See Movie S2 of Supporting Information.

bonding of Cys81– S^- with C6 of cytosine followed by methyl transfer (Figure S3 of Supporting Information).²⁰ (M3): Stepwise methyl transfer catalyzed by proton transfer from Glu119 to N3 of cytosine; the protonation promotes S–C6 covalent bond formation and is concerted with it; methyl transfer follows (Figure S4 of Supporting Information).⁷⁸ (M4): Deprotonation of Cys81–SH before the methyl transfer reaction; Cys81–SH is deprotonated by the nonbridging phosphate oxygen on the 3' side of the target cytosine, via a mediating water;²⁹ then the concerted methyl transfer reaction proceeds (Figure S5 of Supporting Information). (M5): Direct nucleophilic attack of the C5 on the methyl group of AdoMet but with Cys81 protonated (Cys81–SH). This mechanism tests the possibility that the role of Cys81 is to electrostatically foster the activation of C5 for the methyl transfer step, without forming a covalent bond with cytosine C6 (Figure S6 of Supporting Information). Our motivation (M4 and M5) was that the protonation state of the cysteine in the reactant complex is an open question.^{29,37}

For the cytosine C5 proton β -elimination, we investigated several possibilities for the proton-abstracting base. (E1): The leaving Cys81– S^- directly abstracts the proton (Figure S7 of Supporting Information).⁷⁹ (E2): Cys81– S^- abstracts the proton through a water bridge (Figure S8 of Supporting Information).²⁹ (E3): The nonbridging phosphate oxygen on the 3' side of the target cytosine abstracts the proton, via a two-water bridge (Figure S9 of Supporting Information).²⁴ (E4): A proton wire water channel provides a OH^- as the base (Figure 3A).²⁸

Our wide surveys have indicated that the energetically most favored mechanism entails methyl transfer that is concerted

with covalent bonding of Cys81– S^- and cytosine C6 and that the base for proton abstraction is an OH^- provided by a proton wire through a water channel. The mechanism also reveals a dynamic proton transfer between Glu119 and cytosine N3 during the transition state of the methyl transfer step.

Methyl Transfer Is Concerted with Michael Addition and Catalyzed by Proton Transfer from Glu119 in the Transition State. We have determined that the first, methyl transfer step in our preferred mechanism for the reaction is a nucleophilic attack of the C5 on the methyl group of AdoMet, with concerted catalytic attack by the Cys81– S^- group at the C6 position of the target cytosine to form a 5-methyl-6-Cys81-S-5,6-dihydrocytosine intermediate (Figure 2A). It is noteworthy that the Cys81– S^- , which is highly nucleophilic, attacks the cytosine C6 spontaneously. A free energy profile for the methyl transfer step was determined by ab initio QM/MM-MD simulation and umbrella sampling as shown in Figure 2B, determined by employing 21 umbrella windows along the reaction coordinate, each simulated for 30 ps with B3LYP (6-31G*) QM/MM-MD calculations. The calculated free energy activation barrier for the methylation reaction is 15.8 ± 0.3 kcal/mol. Unrestrained 1–2 ps QM/MM MD simulations of 39 snapshots from the transition state structures showed that they relaxed to the reactant and intermediate with almost equal probability, indicating that a real transition state had been located (Figure S10 of Supporting Information). The intermediate 1 (I1) is an energetically very stable state, which has a much lower free energy (–30.4 kcal/mol) than the reactant state.

We obtained the active site geometry of the determined reactant, transition state, and intermediate in the initial

methylation step, as shown in Figure 2A and Movie S1 of Supporting Information. In the reactant state, the Cys81-S⁻ is 3.2 Å away from the C6 of the cytosine ring and is well positioned for nucleophilic attack on C6 to form a covalently bonded adduct between Cys81-S⁻ and cytosine C6. The methyl donor AdoMet is also well situated for an in-line nucleophilic attack by C5 of the activated cytosine, with a CH₃-C5 distance of 3.3 Å. At the transition state, the AdoMet S-CH₃ distance has stretched from its normal covalent bond distance of 1.8 Å to 2.2 Å, and the CH₃-C5 distance has shortened to 2.3 Å. In addition, the distance between cytosine C6 and Cys81-S⁻ has shortened to 2.2 Å. The 30 ps QM/MM-MD simulation of the transition state structure showed fluctuations in the S-C6 distance that occasionally reached ~3 Å (Figure S11 of Supporting Information), indicating that this bond can episodically reverse and reform, consistent with experimental evidence.³⁷ As described below, the Glu119 carboxylic acid hydrogen is hydrogen bonded to N3 of cytosine in the reactant and transition state. Notably, the 30 ps QM/MM-MD simulation for the transition state showed that the Glu119 carboxylic acid hydrogen spontaneously fluctuates between being positioned on the Glu119 with a hydrogen bond to cytosine N3 and being covalently bonded to the cytosine N3, with constant heavy atom to heavy atom distance (Figure 2C). When the methyl group has completely transferred to the cytosine, we obtain the energetically very stable intermediate 1 (I1).

We analyzed hydrogen bonding interactions between certain active site amino acid residues and substrate. Glu119, Arg163, and Arg165 are conserved residues.^{76,77} Mutating Glu119⁷³ and Arg165⁷⁵ reduces the overall catalytic rate by several orders of magnitude. While there are no mutation studies for Arg163, it has been implicated as playing a role in the methylation process.^{24,28,29,75} These amino acids may be essential for maintaining the target cytosine in the flipped-out position, and/or they may play a role in the chemical reaction directly.⁷³ We monitored hydrogen bonding interactions between these residues and the substrate for the key states in our preferred mechanism. Hydrogen bond occupancies are shown in Figure 4, and time-dependence of distances and angles are given in Figure S12 of Supporting Information. We find close and stable hydrogen bonds between Glu119 and cytosine N3 as well as N4 in the reactant state; in the transition state the Glu119 carboxylic acid hydrogen spontaneously and reversibly transfers to N3 as described above (Figure 2C); it is present as a

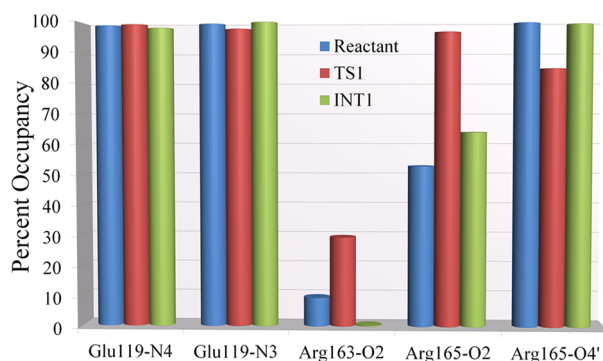


Figure 4. Hydrogen bond occupancies along the 30 ps QM/MM-MD simulation for each key state in the methyl transfer step. Hydrogen bond criteria: heavy atom to heavy atom distance less than 3.4 Å and heavy atom – H – heavy atom angle of 180° ± 45°.

hydrogen bond in the intermediate state. This Glu119 was protonated in the reactant state for all investigated mechanisms because crystal structures of *M.HhaI* complexed with unmethylated or hemimethylated DNA together with S-adenosyl-L-homocysteine (AdoHcy) show heavy atom to heavy atom distances between Glu119 carboxylic acid oxygen (O^{e2}) and cytosine N3 that strongly suggest hydrogen bonding, with distances of 3.22 Å, 2.75 Å, and 2.97 Å for the three obtained structures.²⁴ Protonation allows hydrogen bonding with or proton transfer to cytosine N3. The stable hydrogen bond we observed explains the increase in pK_a in the enzyme, as the energetic cost of protonation of the Glu119 is compensated by the formation of the hydrogen bond.⁸⁰ Hydrogen bonding between Arg163 and cytosine O2 is weak in all three states, but stabilizing electrostatic interactions from near-hydrogen bonding orientations are present in all states (Figure S12 of Supporting Information). Arg165 also maintains hydrogen bonds or electrostatic interactions that are near-hydrogen bonding with cytosine O2 and O4' in the reactant, transition state, and intermediate.

Other mechanistic possibilities for the methyl transfer that were investigated are fully detailed in Supporting Information and Figures S3–S6 of Supporting Information. They were all unfavorable, providing unstable intermediates or much higher energy barriers.

β-Elimination Uses a Crystal Water-Derived OH⁻ as Base. The nature of the base and mechanism for abstraction of the C5 proton has been the subject of considerable interest. We thoroughly explored four different possibilities, detailed above, beginning with the intermediate 1 (I1) from the methyl transfer step (Figure 2A). One possibility for the base, suggested by Zhang and Bruice,²⁸ is that the base is a nearby OH⁻; a solvent water channel mediates the proton interchange to provide the OH⁻, and it was pointed out that the production of this OH⁻ would cost about 12 kcal/mol.⁴ Of the mechanisms that we explored, this mechanism provided the lowest free energy profile. Moreover, we determined that the OH⁻ could be provided by a proton wire to bulk water. Using 10 ns molecular dynamics simulations, we observed a stable channel of water emanating from the approximate position of WAT1 (Figure 1B) to the enzyme surface and bulk water. The channel is shown in Figure 3A for a random snapshot of the MD. It is noteworthy that WAT1 and WAT3 in Figure 3A are in positions of crystal waters,^{24,39} and they remained there stably throughout the MD simulation. Other crystal and solvent waters may provide different proton wire channels. WAT1 is conserved in a number of crystal structures of *M.HhaI*.^{24,75,81} We replaced the water at the WAT1 position with a OH⁻, and the system is referred to as intermediate 2 (I2). The mechanism for proton abstraction through OH⁻ is shown in Figure 3B and Movie S2 of Supporting Information. Our obtained free energy profile using B3LYP (6-31G*) QM/MM-MD simulations with 30 umbrella sampling windows, each calculated for 30 ps, is shown in Figure 3C. A barrier of 8.7 ± 0.9 kcal/mol was obtained. Together with the 12 kcal/mol required to produce the OH⁻, the barrier is 20.7 kcal/mol, making the proton abstraction the rate limiting step.

Figure 3B shows that in the intermediate state 2 (I2) the OH⁻ is 3.2 Å away from the C5 proton, while in the transition state, the distance has shortened to 1.4 Å, and the C5 proton has begun to leave the C5 with a distance of 1.3 Å. In the intermediate and transition state, the bond between cytosine C6 and Cys81-S⁻ remains intact (1.9 Å) until the C5-HS

bond is broken, and then the Cys81 detaches and releases the methylated cytosine and AdoHcy. The complete bond length analysis for the process which reveals this dynamic is shown in Figure S13 of Supporting Information. Our hydrogen bond analyses (Figure 5) show that as in the methylation step,

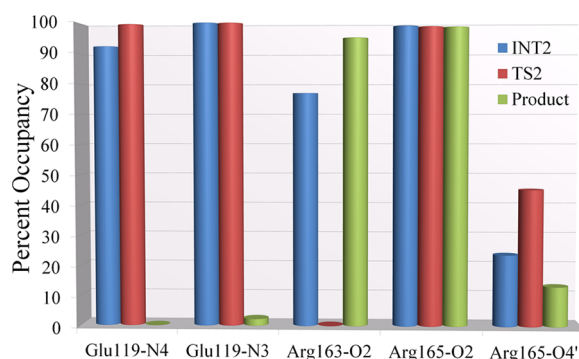


Figure 5. Hydrogen bond occupancies along the 30 ps QM/MM-MD simulation for each key state in the β -elimination step. Hydrogen bond criteria are the same as in Figure 4.

hydrogen bonding or electrostatic interactions due to near-hydrogen bonding orientations (Figure S12 of Supporting Information) are present in intermediate, transition state, and product except for Glu119 in the product. In this case, cytosine N3 remains hydrogen bonded through a water, but cytosine N4 is no longer close to Glu119, initiating the release of the methylated cytosine.

Other mechanistic possibilities that we investigated for the proton abstraction had much higher energy barriers. These are detailed in full in Supporting Information and Figures S7–S9 of Supporting Information.

DISCUSSION

We investigated extensively the methylation reaction catalyzed by *M.HhaI*, exploring many mechanistic possibilities; we used for the first time state-of-the-art ab initio QM/MM-MD methods in which the chemically reacting moieties are treated by high level ab initio QM methods, while the surrounding enzyme is treated by classical MM. A key feature of our approach is that the dynamics of the enzyme active site and its surroundings are treated on an equal footing. The free energy profile along the reaction coordinate is obtained from a series of biased simulations,⁶³ which are employed to enhance the sampling of lower probability states, with the weighted histogram analysis method (WHAM).^{67–69} This advanced approach provides a first-principle QM description of the chemical reaction. Furthermore, it adequately accounts for the biological environment. Importantly, it takes a balanced account of the fluctuations of the reaction active site and the surrounding enzyme system. Mechanisms of various enzymes that are consistent with experimental data have been determined with this powerful method.^{30–36}

We investigated mechanistic issues that have been of significant interest, but are not definitively resolved. For the methyl transfer step of the reaction, we explored whether the formation of the Michael adduct between conserved Cys81–S[−] and cytosine C6 and the transfer of the methyl group are concerted or stepwise, as there are conflicting views.^{20,28,29,78} We also investigated the possibility that the conserved residue Glu119 donates a proton to cytosine N3 to promote the

formation of the covalent adduct.⁷⁸ In addition, we considered the possibility that the Cys81–SH thiol is deprotonated to the Cys81–S[−] thiolate through proton transfer to a nonbridging phosphate oxygen.²⁹ Also, we investigated a mechanism in which the Cys81–SH, the thiol protonated state—which cannot form a covalent adduct—might provide nonbonded electrostatic stabilization to facilitate the methyl transfer. For the proton elimination step, we considered the following potential bases: (1) the leaving thiolate of Cys81 acts as the base either directly, or (2) through a water;²⁹ (3) the 3′ nonbridging phosphate oxygen of the target cytosine acts as the base via two waters; and (4) an OH[−] derived from a crystal water acts as the base, utilizing a water channel as suggested by Zhang and Bruice.²⁸ While our extensive investigations provided a clearly favored mechanism, it remains a possibility, as always in computational investigations of reaction energy surfaces, that there are other pathways that were not found.

Our energetically preferred mechanism (Movie S1, Supporting Information) involves a methylation reaction in which spontaneous attack of Cys81–S[−] to form a Michael adduct with cytosine C6 is concerted with methyl transfer, in agreement with Zhang and Bruice.²⁸ Our bond length analyses (Figure S11 of Supporting Information) show that the covalent bond between Cys81–S[−] and cytosine C6 forms rapidly, and QM/MM-MD simulations show that the bond can form and break reversibly, consistent with kinetic studies.³⁷ An important finding is the observation of proton transfer from Glu119 to cytosine N3, spontaneously and reversibly, during the transition state for the methylation step; this transfer indicates the catalytic participation of Glu119 in the chemical reaction, as proposed by Verdine.⁷⁸ The conserved Glu119 is protonated and hydrogen bonds with cytosine N3 and N4 throughout the whole reaction (Figures 4 and 5) until the release of the product. The increase in pK_a of the Glu in the enzyme is explained by the stable hydrogen bond to cytosine N3, as its protonation allows the formation of the hydrogen bond.⁸⁰ The hydrogen bonds between Glu119 and cytosine provide electrostatic support for the mechanism, particularly by withdrawing electrons in the reactant to make C6 more positive for attack by Cys81–S[−], and these hydrogen bonds have been strongly suggested by crystal structures.²⁴

For the proton elimination step (Movie S2, Supporting Information), our favored mechanism utilizes as base a OH[−] that has migrated to the active site through a proton wire involving a channel of waters between the active site and bulk water. Simulations have shown that proton transfer between adjacent water molecules in a proton wire is spontaneous and very fast.⁸² The key water that provided the OH[−] is in the position of a crystal water (Figures 1B and 3A), and other crystal waters may participate in the proton wire. We found that the proton abstraction step is rate-limiting when factoring in the energetic cost, about 12 kcal/mol,^a of generating the OH[−] through the proton wire. This is chemically reasonable since the proton abstraction involves a *syn* β -elimination; the proton leaves on the same face of the cytosine ring as the Cys81–S[−], which is sterically crowded and hence slow.⁸³ Furthermore, the difficult *syn*-elimination requires a strong base for the proton abstraction, which supports the OH[−] as base in our preferred mechanism. The total barrier of 20.7 kcal/mol for this rate limiting step is in good agreement with measured *k*_{cat} values for the overall methyl transfer reaction (0.02 S^{−1} to 0.09 S^{−1},^{20,84,85} which corresponds to 19.0–20.0 kcal/mol according to

transition state theory: $k_{\text{cat}}(T) = (k_{\text{B}}T/h) e^{-(\Delta G^\ddagger/RT)}$ (where k_{cat} is the catalytic rate-constant, k_{B} is the Boltzmann constant, h is the Planck constant, R is the universal gas constant, T is the temperature (300 K), and ΔG^\ddagger is the free energy of activation).

The roles of the conserved residues Glu119, Arg163, and Arg165 are further elucidated in our hydrogen bond analyses. All of them provide stabilizing hydrogen bonding (Figures 4 and 5) or near-hydrogen bonding electrostatic interactions (Figure S12 of Supporting Information) throughout both the methyl transfer and β -elimination steps except for Glu119 in the final product, which has moved away to initiate the release. In addition to stabilizing the flipped out position of the substrate cytosine in the enzyme reactive site pocket,^{73,75} their electrostatic impact in the reactant state in withdrawing electrons from the target cytosine makes C6 more positive for attack by Cys81-S⁻. Furthermore, we demonstrated that the Glu119 carboxylic acid proton is reversibly transferred to cytosine N3 in the transition state for methylation, and thus this residue participates in the chemical reaction.⁷⁸

CONCLUSION

We have utilized state-of-the-art ab initio QM/MM-MD simulations, exploring multiple mechanistic possibilities, to fully characterize the reaction mechanism of a representative DNA cytosine methyltransferase. From prokaryotes to mammals, all of these enzymes share mechanistic features. They play critical roles in governing epigenetically the function of the genome. Furthermore, their function is misregulated in many human diseases, and targeting them pharmacologically is currently a very important research direction. Molecular understanding of the mechanism is required to effectively target cytosine methyltransferases with aberrant activity. Our results provide for the first time a complete structural and thermodynamic characterization of the full reaction profile. We provide an atomistic characterization of the reaction dynamics and a determination of the roles of key protein residues in the active site. We show how a conserved Glu residue chemically promotes the methyl transfer reaction during the transition state and how a conserved crystal water provides a critical OH⁻ base needed for β -elimination of the C5 proton, via a proton wire through a water channel. The complete depiction of the structural, dynamic, and thermodynamic elements in the cytosine methyltransferase reaction should facilitate the design of therapeutic inhibitors, particularly novel and more potent transition state analogue inhibitors that are of interest for drug design as transition states become fully characterized.⁸⁶

ASSOCIATED CONTENT

Supporting Information

Additional details regarding MD simulation protocol and other tested mechanisms. Protonation state of charged residue assignments (Table S1) and force field parameters (Table S2). Figures S1–S14 and Movies S1–S2 as described in the text. This material is available free of charge via the Internet at <http://pubs.acs.org>.

AUTHOR INFORMATION

Corresponding Author

*(Y.Z.) Phone: (212) 998-7882. Fax (212) 995-4475. E-mail: yingkai.zhang@nyu.edu. (S.B.) Phone: (212) 998-8231. Fax (212) 995-4015. E-mail: broyde@nyu.edu.

Funding

The research reported in this publication was supported by National Institutes of Health (NIH) [R01-CA-75449 and R01-CA-28038 to S.B., and R01-GM079223 to Y.Z.] and NSF [CHE-CAREER-0448156 to Y.Z.]. The content is solely the responsibility of the authors and does not necessarily represent the official views of the National Cancer Institute or the National Institutes of Health.

Notes

The authors declare no competing financial interest.

ACKNOWLEDGMENTS

This work used computational resources of the Extreme Science and Engineering Discovery Environment (XSEDE), which is supported by National Science Foundation Grant MCB060037 to S.B. We also gratefully acknowledge computational resources provided by the Multipurpose High Performance Computing resource of New York University (NYU-ITS). The content is solely the responsibility of the authors and does not necessarily represent the official views of the National Cancer Institute or the National Institutes of Health.

ABBREVIATIONS

QM/MM-MD, quantum mechanical/molecular mechanical - molecular dynamics; M.HhaI, methyltransferase HhaI; Ado-Met, S-adenosyl-L-methionine; DNMT1, DNA methyltransferase 1; AdoHcy, S-adenosyl-L-homocysteine

ADDITIONAL NOTE

^aIn pure water, [H₂O] is 55.6 M, [OH⁻] is 10⁻⁷ M at pH = 7.0. Thus, the probability of observing an OH⁻ versus a water molecule is 10⁻⁷/55.6. Therefore, the free energy difference ΔG between OH⁻ and H₂O at pH = 7.0 is: $\Delta G = -RT \ln K_{\text{eq}} = -0.5961 \times \ln(10^{-7}/55.6) = 12.0 \text{ kcal/mol}$.

REFERENCES

- (1) Mueller, W. C., and von Deimling, A. (2009) Gene regulation by methylation. *Recent Results Cancer Res.* 171, 217–239.
- (2) Li, E., Bestor, T. H., and Jaenisch, R. (1992) Targeted mutation of the DNA methyltransferase gene results in embryonic lethality. *Cell* 69, 915–926.
- (3) Okano, M., Bell, D. W., Haber, D. A., and Li, E. (1999) DNA methyltransferases Dnmt3a and Dnmt3b are essential for de novo methylation and mammalian development. *Cell* 99, 247–257.
- (4) Panning, B., and Jaenisch, R. (1996) DNA hypomethylation can activate Xist expression and silence X-linked genes. *Genes Dev.* 10, 1991–2002.
- (5) Hore, T. A., Rapkins, R. W., and Graves, J. A. (2007) Construction and evolution of imprinted loci in mammals. *Trends Genet.* 23, 440–448.
- (6) Jeltsch, A. (2002) Beyond Watson and Crick: DNA methylation and molecular enzymology of DNA methyltransferases. *ChemBiochem* 3, 274–293.
- (7) Jones, P. A. (2012) Functions of DNA methylation: islands, start sites, gene bodies and beyond. *Nat. Rev. Genet.* 13, 484–492.
- (8) Goll, M. G., and Bestor, T. H. (2005) Eukaryotic cytosine methyltransferases. *Annu. Rev. Biochem.* 74, 481–514.
- (9) Robertson, K. D. (2005) DNA methylation and human disease. *Nat. Rev. Genet.* 6, 597–610.
- (10) Kulis, M., and Esteller, M. (2010) DNA methylation and cancer. *Adv. Genet.* 70, 27–56.
- (11) Kobow, K., and Blumcke, I. (2012) The emerging role of DNA methylation in epileptogenesis. *Epilepsia* 53, 11–20.
- (12) Subach, O. M., Baskunov, V. B., Darii, M. V., Maltseva, D. V., Alexandrov, D. A., Kirsanova, O. V., Kolbanovskiy, A., Kolbanovskiy,

M., Johnson, F., Bonala, R., Geacintov, N. E., and Gromova, E. S. (2006) Impact of benzo[a]pyrene-2'-deoxyguanosine lesions on methylation of DNA by SssI and HhaI DNA methyltransferases. *Biochemistry* 45, 6142–6159.

(13) Lukashevich, O. V., Baskunov, V. B., Darii, M. V., Kolbanovskiy, A., Baykov, A. A., and Gromova, E. S. (2011) Dnmt3a-CD is less susceptible to bulky benzo[a]pyrene diol epoxide-derived DNA lesions than prokaryotic DNA methyltransferases. *Biochemistry* 50, 875–881.

(14) Guza, R., Kotandeniya, D., Murphy, K., Dissanayake, T., Lin, C., Giambasu, G. M., Lad, R. R., Wojciechowski, F., Amin, S., Sturla, S. J., Hudson, R. H., York, D. M., Jankowiak, R., Jones, R., and Tretyakova, N. Y. (2011) Influence of C-5 substituted cytosine and related nucleoside analogs on the formation of benzo[a]pyrene diol epoxide-dG adducts at CG base pairs of DNA. *Nucleic Acids Res.* 39, 3988–4006.

(15) Medina-Franco, J. L., and Caulfield, T. (2011) Advances in the computational development of DNA methyltransferase inhibitors. *Drug Discovery Today* 16, 418–425.

(16) Ren, J., Singh, B. N., Huang, Q., Li, Z. F., Gao, Y., Mishra, P., Hwa, Y. L., Li, J. P., Dowdy, S. C., and Jiang, S. W. (2011) DNA hypermethylation as a chemotherapy target. *Cell. Signal.* 23, 1082–1093.

(17) Xu, F., Mao, C., Ding, Y., Rui, C., Wu, L., Shi, A., Zhang, H., Zhang, L., and Xu, Z. (2010) Molecular and Enzymatic Profiles of Mammalian DNA Methyltransferases: Structures and Targets for Drugs. *Curr. Med. Chem.* 17, 4052–4071.

(18) Dhe-Paganon, S., Syeda, F., and Park, L. (2011) DNA methyltransferase 1: regulatory mechanisms and implications in health and disease. *Int. J. Biochem. Mol. Biol.* 2, 58–66.

(19) Ceccaldi, A., Rajavelu, A., Ragozin, S., Senamaud-Beaufort, C., Bashtrykov, P., Testa, N., Dali-Ali, H., Maulay-Bailly, C., Amand, S., Guianvarc'h, D., Jeltsch, A., and Arimondo, P. B. (2013) Identification of Novel Inhibitors of DNA Methylation by Screening of a Chemical Library. *ACS Chem. Biol.* 8, 543–548.

(20) Wu, J. C., and Santi, D. V. (1987) Kinetic and catalytic mechanism of HhaI methyltransferase. *J. Biol. Chem.* 262, 4778–4786.

(21) Sankpal, U. T., and Rao, D. N. (2002) Structure, function, and mechanism of HhaI DNA methyltransferases. *Crit. Rev. Biochem. Mol. Biol.* 37, 167–197.

(22) Cheng, X. D., and Blumenthal, R. M. (2008) Mammalian DNA methyltransferases: A structural perspective. *Structure* 16, 341–350.

(23) Song, J., Teplova, M., Ishibe-Murakami, S., and Patel, D. J. (2012) Structure-based mechanistic insights into DNMT1-mediated maintenance DNA methylation. *Science* 335, 709–712.

(24) O'Gara, M., Klimasauskas, S., Roberts, R. J., and Cheng, X. D. (1996) Enzymatic C5-cytosine methylation of DNA: Mechanistic implications of new crystal structures for HhaI methyltransferase-DNA-AdoHcy complexes. *J. Mol. Biol.* 261, 634–645.

(25) Klimasauskas, S., Kumar, S., Roberts, R. J., and Cheng, X. D. (1994) HhaI Methyltransferase Flips Its Target Base out of the DNA Helix. *Cell* 76, 357–369.

(26) Zhou, L., Cheng, X., Connolly, B. A., Dickman, M. J., Hurd, P. J., and Hornby, D. P. (2002) Zebularine: A novel DNA methylation inhibitor that forms a covalent complex with DNA methyltransferases. *J. Mol. Biol.* 321, 591–599.

(27) Fahy, J., Jeltsch, A., and Arimondo, P. B. (2012) DNA methyltransferase inhibitors in cancer: a chemical and therapeutic patent overview and selected clinical studies. *Expert Opin. Ther. Pat.* 22, 1427–1442.

(28) Zhang, X., and Bruice, T. C. (2006) The mechanism of M.HhaI DNA C5 cytosine methyltransferase enzyme: a quantum mechanics/molecular mechanics approach. *Proc. Natl. Acad. Sci. U. S. A.* 103, 6148–6153.

(29) Zangi, R., Arrieta, A., and Cossio, F. P. (2010) Mechanism of DNA methylation: the double role of DNA as a substrate and as a cofactor. *J. Mol. Biol.* 400, 632–644.

(30) Hu, P., Wang, S. L., and Zhang, Y. K. (2008) Highly Dissociative and Concerted Mechanism for the Nicotinamide Cleavage Reaction in

Sir2Tm Enzyme Suggested by Ab Initio QM/MM Molecular Dynamics Simulations. *J. Am. Chem. Soc.* 130, 16721–16728.

(31) Wu, R. B., Wang, S. L., Zhou, N. J., Cao, Z. X., and Zhang, Y. K. (2010) A Proton-Shuttle Reaction Mechanism for Histone Deacetylase 8 and the Catalytic Role of Metal Ions. *J. Am. Chem. Soc.* 132, 9471–9479.

(32) Zhou, Y. Z., Wang, S. L., and Zhang, Y. K. (2010) Catalytic Reaction Mechanism of Acetylcholinesterase Determined by Born-Oppenheimer Ab Initio QM/MM Molecular Dynamics Simulations. *J. Phys. Chem. B* 114, 8817–8825.

(33) Smith, G. K., Ke, Z. H., Guo, H., and Hengge, A. C. (2011) Insights into the Phosphoryl Transfer Mechanism of Cyclin-Dependent Protein Kinases from ab Initio QM/MM Free-Energy Studies. *J. Phys. Chem. B* 115, 13713–13722.

(34) Lior-Hoffmann, L., Wang, S. L., Geacintov, N. E., Broyde, S., and Zhang, Y. K. (2012) Preferred WMSA catalytic mechanism of the nucleotidyl transfer reaction in human DNA polymerase kappa elucidates error-free bypass of a bulky DNA lesion. *Nucleic Acids Res.* 40, 9193–9205.

(35) Sirin, G. S., Zhou, Y. Z., Lior-Hoffmann, L., Wang, S. L., and Zhang, Y. K. (2012) Aging Mechanism of Soman Inhibited Acetylcholinesterase. *J. Phys. Chem. B* 116, 12199–12207.

(36) Rooklin, D. W., Lu, M., and Zhang, Y. K. (2012) Revelation of a Catalytic Calcium-Binding Site Elucidates Unusual Metal Dependence of a Human Apyrase. *J. Am. Chem. Soc.* 134, 15595–15603.

(37) Svedruzic, Z. M., and Reich, N. O. (2004) The mechanism of target base attack in DNA cytosine carbon 5 methylation. *Biochemistry* 43, 11460–11473.

(38) Berman, H. M., Battistuz, T., Bhat, T. N., Bluhm, W. F., Bourne, P. E., Burkhardt, K., Iype, L., Jain, S., Fagan, P., Marvin, J., Padilla, D., Ravichandran, V., Schneider, B., Thanki, N., Weissig, H., Westbrook, J. D., and Zardecki, C. (2002) The Protein Data Bank. *Acta Crystallogr., Sect. D: Biol. Crystallogr.* 58, 899–907.

(39) Kumar, S., Horton, J. R., Jones, G. D., Walker, R. T., Roberts, R. J., and Cheng, X. (1997) DNA containing 4'-thio-2'-deoxycytidine inhibits methylation by HhaI methyltransferase. *Nucleic Acids Res.* 25, 2773–2783.

(40) Case, D. A., Darden, T. A., Cheatham, T. E., III, Simmerling, C. L., Wang, J., Duke, R. E., Luo, R., Crowley, M., Walker, R. C., Zhang, W., Merz, K. M., Wang, B., Hayik, S., Roitberg, A., Seabra, G., Kolossvary, I., Wong, K. F., Paesani, F., Vanicek, J., Wu, X., Brozell, S. R., Steinbrecher, T., Gohlke, H., Yang, L., Tan, C., Mongan, J., Hornak, V., Cui, G., Mathews, D. H., Seetin, M. G., Sagui, C., Babin, V., and Kollman, P. A. (2008) AMBER 10, University of California, San Francisco.

(41) Gordon, J. C., Myers, J. B., Foltz, T., Shojha, V., Heath, L. S., and Onufriev, A. (2005) H++: a server for estimating pKas and adding missing hydrogens to macromolecules. *Nucleic Acids Res.* 33, W368–371.

(42) Anandakrishnan, R., and Onufriev, A. (2008) Analysis of basic clustering algorithms for numerical estimation of statistical averages in biomolecules. *J. Comput. Biol.* 15, 165–184.

(43) Dolinsky, T. J., Nielsen, J. E., McCammon, J. A., and Baker, N. A. (2004) PDB2PQR: an automated pipeline for the setup of Poisson-Boltzmann electrostatics calculations. *Nucleic Acids Res.* 32, W665–667.

(44) Wang, J. M., Cieplak, P., and Kollman, P. A. (2000) How well does a restrained electrostatic potential (RESP) model perform in calculating conformational energies of organic and biological molecules? *J. Comput. Chem.* 21, 1049–1074.

(45) Cornell, W. D., Cieplak, P., Bayly, C. I., Gould, I. R., Merz, K. M., Ferguson, D. M., Spellmeyer, D. C., Fox, T., Caldwell, J. W., and Kollman, P. A. (1995) A 2nd Generation Force-Field for the Simulation of Proteins, Nucleic-Acids, and Organic-Molecules. *J. Am. Chem. Soc.* 117, 5179–5197.

(46) Hornak, V., Abel, R., Okur, A., Strockbine, B., Roitberg, A., and Simmerling, C. (2006) Comparison of multiple amber force fields and development of improved protein backbone parameters. *Proteins: Struct., Funct. Bioinf.* 65, 712–725.

- (47) Perez, A., Marchan, I., Svozil, D., Sponer, J., Cheatham, T. E., Laughton, C. A., and Orozco, M. (2007) Refinement of the AMBER force field for nucleic acids: Improving the description of alpha/gamma conformers. *Biophys. J.* 92, 3817–3829.
- (48) Markham, G. D., Norrby, P. O., and Bock, C. W. (2002) S-Adenosylmethionine conformations in solution and in protein complexes: Conformational influences of the sulfonium group. *Biochemistry* 41, 7636–7646.
- (49) Petersson, G. A., Bennett, A., Tensfeldt, T. G., Allaham, M. A., Shirley, W. A., and Mantzaris, J. (1988) A Complete Basis Set Model Chemistry 0.1. The Total Energies of Closed-Shell Atoms and Hydrides of the 1st-Row Elements. *J. Chem. Phys.* 89, 2193–2218.
- (50) Petersson, G. A., and Allaham, M. A. (1991) A Complete Basis Set Model Chemistry 0.2. Open-Shell Systems and the Total Energies of the 1st-Row Atoms. *J. Chem. Phys.* 94, 6081–6090.
- (51) Frisch, M. J., Trucks, G. W., Schlegel, H. B., Scuseria, G. E., Robb, M. A., Cheeseman, J. R., Montgomery, J. J. A., Vreven, T., Kudin, K. N., Burant, J. C., Millam, J. M., Iyengar, S. S., Tomasi, J., Barone, V., Mennucci, B., Cossi, M., Scalmani, G., Rega, N., Petersson, G. A., Nakatsuji, H., Hada, M., Ehara, M., Toyota, K., Fukuda, R., Hasegawa, J., Ishida, M., Nakajima, T., Honda, Y., Kitao, O., Nakai, H., Klene, M., Li, X., Knox, J. E., Hratchian, H. P., Cross, J. B., Bakken, V., Adamo, C., Jaramillo, J., Gomperts, R., Stratmann, R. E., Yazyev, O., Austin, A. J., Cammi, R., Pomelli, C., Ochterski, J. W., Ayala, P. Y., Morokuma, K., Voth, G. A., Salvador, P., Dannenberg, J. J., Zakrzewski, V. G., Dapprich, S., Daniels, A. D., Strain, M. C., Farkas, O., Malick, D. K., Rabuck, A. D., Raghavachari, K., Foresman, J. B., Ortiz, J. V., Cui, Q., Baboul, A. G., Clifford, S., Cioslowski, J., Stefanov, B. B., Liu, G., Liashenko, A., Piskorz, P., Komaromi, I., Martin, R. L., Fox, D. J., Keith, T., Al-Laham, M. A., Peng, C. Y., Nanayakkara, A., Challacombe, M., Gill, P. M. W., Johnson, B., Chen, W., Wong, M. W., Gonzalez, C., and Pople, J. A. (2004) *Gaussian 03*, revision D.01, Gaussian, Inc., Wallingford, CT.
- (52) Bayly, C. I., Cieplak, P., Cornell, W. D., and Kollman, P. A. (1993) A Well-Behaved Electrostatic Potential Based Method Using Charge Restraints for Deriving Atomic Charges - the Resp Model. *J. Phys. Chem.* 97, 10269–10280.
- (53) Jorgensen, W. L., Chandrasekhar, J., Madura, J. D., Impey, R. W., and Klein, M. L. (1983) Comparison of Simple Potential Functions for Simulating Liquid Water. *J. Chem. Phys.* 79, 926–935.
- (54) Price, D. J., and Brooks, C. L. (2004) A modified TIP3P water potential for simulation with Ewald summation. *J. Chem. Phys.* 121, 10096–10103.
- (55) Lee, C., Yang, W., and Parr, R. G. (1988) Development of the Colle-Salvetti correlation-energy formula into a functional of the electron density. *Phys. Rev. B* 37, 785–789.
- (56) Becke, A. D. (1998) Density-functional exchange-energy approximation with correct asymptotic behavior. *Phys. Rev. A* 38, 3098–3100.
- (57) Becke, A. D. (1993) Density-Functional Thermochemistry 0.3. The Role of Exact Exchange. *J. Chem. Phys.* 98, 5648–5652.
- (58) Zhang, Y., Lee, T., and Yang, W. (1999) A pseudobond approach to combining quantum mechanical and molecular mechanical methods. *J. Chem. Phys.* 110, 46–54.
- (59) Zhang, Y. K. (2005) Improved pseudobonds for combined ab initio quantum mechanical/molecular mechanical methods. *J. Chem. Phys.* 122, 024114.
- (60) Zhang, Y. K. (2006) Pseudobond ab initio QM/MM approach and its applications to enzyme reactions. *Theor. Chem. Acc.* 116, 43–50.
- (61) Shao, Y., Molnar, L. F., Jung, Y., Kussmann, J., Ochsenfeld, C., Brown, S. T., Gilbert, A. T. B., Slipchenko, L. V., Levchenko, S. V., O'Neill, D. P., DiStasio, R. A., Lochan, R. C., Wang, T., Beran, G. J. O., Besley, N. A., Herbert, J. M., Lin, C. Y., Van Voorhis, T., Chien, S. H., Sodt, A., Steele, R. P., Rassolov, V. A., Maslen, P. E., Korambath, P. P., Adamson, R. D., Austin, B., Baker, J., Byrd, E. F. C., Dachsel, H., Doerksen, R. J., Dreuw, A., Dunietz, B. D., Dutoi, A. D., Furlani, T. R., Gwaltney, S. R., Heyden, A., Hirata, S., Hsu, C. P., Kedziora, G., Khaliullin, R. Z., Klunzinger, P., Lee, A. M., Lee, M. S., Liang, W., Lotan, I., Nair, N., Peters, B., Proynov, E. I., Pieniazek, P. A., Rhee, Y. M., Ritchie, J., Rosta, E., Sherrill, C. D., Simonnet, A. C., Subotnik, J. E., Woodcock, H. L., Zhang, W., Bell, A. T., Chakraborty, A. K., Chipman, D. M., Keil, F. J., Warshel, A., Hehre, W. J., Schaefer, H. F., Kong, J., Krylov, A. I., Gill, P. M. W., and Head-Gordon, M. (2006) Advances in methods and algorithms in a modern quantum chemistry program package. *Phys. Chem. Chem. Phys.* 8, 3172–3191.
- (62) Ponder, J. W. (2004) *TINKER: Software Tools for Molecular Design*, Version 4.2 ed, Washington University in St. Louis, St. Louis, MO.
- (63) Zhang, Y. K., Liu, H. Y., and Yang, W. T. (2000) Free energy calculation on enzyme reactions with an efficient iterative procedure to determine minimum energy paths on a combined ab initio QM/MM potential energy surface. *J. Chem. Phys.* 112, 3483–3492.
- (64) Hu, P., Wang, S. L., and Zhang, Y. K. (2008) How do SET-domain protein lysine methyltransferases achieve the methylation state specificity? Revisited by Ab initio QM/MM molecular dynamics simulations. *J. Am. Chem. Soc.* 130, 3806–3813.
- (65) Hu, H., and Yang, W. T. (2008) Free energies of chemical reactions in solution and in enzymes with ab initio quantum mechanics/molecular mechanics methods. *Annu. Rev. Phys. Chem.* 59, 573–601.
- (66) Beeman, D. (1976) Some Multistep Methods for Use in Molecular-Dynamics Calculations. *J. Comput. Phys.* 20, 130–139.
- (67) Kumar, S., Bouzida, D., Swendsen, R. H., Kollman, P. A., and Rosenberg, J. M. (1992) The Weighted Histogram Analysis Method for Free-Energy Calculations on Biomolecules. I. The Method. *J. Comput. Phys.* 13, 1011–1021.
- (68) Souaille, M., and Roux, B. (2001) Extension to the weighted histogram analysis method: combining umbrella sampling with free energy calculations. *Comput. Phys. Commun.* 135, 40–57.
- (69) Ferrenberg, A. M., and Swendsen, R. H. (1988) New Monte-Carlo Technique for Studying Phase-Transitions. *Phys. Rev. Lett.* 61, 2635–2638.
- (70) Merkiene, E., and Klimasauskas, S. (2005) Probing a rate-limiting step by mutational perturbation of AdoMet binding in the HhaI methyltransferase. *Nucleic Acids Res.* 33, 307–315.
- (71) O'Gara, M., Roberts, R. J., and Cheng, X. D. (1996) A structural basis for the preferential binding of hemimethylated DNA by HhaI DNA methyltransferase. *J. Mol. Biol.* 263, 597–606.
- (72) Cheng, X. D., Kumar, S., Posfai, J., Pflugrath, J. W., and Roberts, R. J. (1993) Crystal-Structure of the HhaI DNA Methyltransferase Complexed with S-Adenosyl-L-Methionine. *Cell* 74, 299–307.
- (73) Shieh, F. K., and Reich, N. O. (2007) AdoMet-dependent methyl-transfer: Glu(119) is essential for DNA c5-cytosine methyltransferase M.HhaI. *J. Mol. Biol.* 373, 1157–1168.
- (74) Youngblood, B., Shieh, F. K., Buller, F., Bullock, T., and Reich, N. O. (2007) S-Adenosyl-L-methionine-dependent methyl transfer: Observable precatalytic intermediates during DNA cytosine methylation. *Biochemistry* 46, 8766–8775.
- (75) Shieh, F. K., Youngblood, B., and Reich, N. O. (2006) The role of Arg165 towards base flipping, base stabilization and catalysis in M.HhaI. *J. Mol. Biol.* 362, 516–527.
- (76) Kumar, S., Cheng, X. D., Klimasauskas, S., Mi, S., Posfai, J., Roberts, R. J., and Wilson, G. G. (1994) The DNA (Cytosine-5) Methyltransferases. *Nucleic Acids Res.* 22, 1–10.
- (77) Posfai, J., Bhagwat, A. S., Posfai, G., and Roberts, R. J. (1989) Predictive Motifs Derived from Cytosine Methyltransferases. *Nucleic Acids Res.* 17, 2421–2435.
- (78) Chen, L., Macmillan, A. M., and Verdine, G. L. (1993) Mutational Separation of DNA-Binding from Catalysis in a DNA Cytosine Methyltransferase. *J. Am. Chem. Soc.* 115, 5318–5319.
- (79) Verdine, G. L. (1994) The flip side of DNA methylation. *Cell* 76, 197–200.
- (80) Cleland, W. W., Perry, A. F., and Gerlt, J. A. (1998) The low barrier hydrogen bond in enzymatic catalysis. *J. Biol. Chem.* 273, 25529–25532.

- (81) O'Gara, M., Horton, J. R., Roberts, R. J., and Cheng, X. (1998) Structures of HhaI methyltransferase complexed with substrates containing mismatches at the target base. *Nat. Struct. Biol.* 5, 872–877.
- (82) Pomes, R., and Roux, B. (1996) Structure and dynamics of a proton wire: A theoretical study of H⁺ translocation along the single-file water chain in the gramicidin a channel. *Biophys. J.* 71, 19–39.
- (83) Morrison, R. T., and Boyd, R. N. (1992) *Stereochemistry II. Stereoselective and Stereospecific Reactions, in Organic Chemistry*, 6th ed., p 377, Prentice-Hall, New Delhi.
- (84) Lindstrom, W. M., Jr., Flynn, J., and Reich, N. O. (2000) Reconciling structure and function in HhaI DNA cytosine-C-5 methyltransferase. *J. Biol. Chem.* 275, 4912–4919.
- (85) Vilkaitis, G., Merkiene, E., Serva, S., Weinhold, E., and Klimasauskas, S. (2001) The mechanism of DNA cytosine-5 methylation. Kinetic and mutational dissection of Hhai methyltransferase. *J. Biol. Chem.* 276, 20924–20934.
- (86) Schramm, V. L. (2011) Enzymatic transition states, transition-state analogs, dynamics, thermodynamics, and lifetimes. *Annu. Rev. Biochem.* 80, 703–732.